

Graphene-containing plasma: a medium for the coherent extreme ultraviolet light generation

R. A. Ganeev¹), M. Suzuki, M. Baba, Sh. Yoneya, H. Kuroda

Ophthalmology and Advanced Laser Medical Center, Saitama Medical University, 350-0495 Saitama, Japan

Submitted 15 July 2014

We demonstrate the high-order harmonic generation of femtosecond pulses in the laser ablation plume containing the graphene nanoparticles. The harmonics up to the 33rd order were observed. The presence of graphene nanoparticles in the laser plasma was confirmed during the analysis of ablation debris. The comparative studies of harmonic generation from the ablation of graphene, carbon nanotubes, and diamond nanoparticles showed the advanced properties of the latter medium.

DOI: 10.7868/S0370274X14190047

The unique optical and nonlinear optical properties of graphene have been in the centre of various recent theoretical and experimental studies [1–7]. Particularly, a new scheme based on bilayer graphene as a nonlinear optical material was proposed by Wu et al. [3] with an extremely large second-order optical susceptibility ($\chi^{(2)} \sim 10^5 \text{ pm} \cdot \text{V}^{-1}$). Recent experiments of Hendry et al. have shown that the nonlinear generation of laser harmonics could be detected even through single layer graphene [6]. The theory of the nonlinear electromagnetic response of graphene has been developed by Mikhailov [2] and Ishikawa [7]. Gullans et al. [4] have shown that it is possible to realize significant nonlinear optical interactions at the few photon level in graphene nanostructures. The high-order harmonic generation (HHG) from a graphene sheet exposed to intense femtosecond laser pulses has been theoretically studied by Sørgård et al. [5] based on the three-step model of HHG. They predicted that graphene may generate more intense harmonic signals than gas-phase atoms or molecules and serve as a useful tool for selective harmonic generation when exposed to an intense driving laser field, though the experimental evidence of HHG in this medium has not been reported.

In the meantime, the laser ablation based HHG experiments have been advanced towards the molecules of increasing complexity such as fullerenes [8] and carbon nanotubes [9]. Previous estimates of similar plasma structures produced on the surfaces of powdered nanomaterials during laser ablation have shown that the concentration of particles becomes close to $\sim 10^{17} \text{ cm}^{-3}$ [8], which should be enough to induce the nonlinear optical processes.

The purpose and advantage of generating harmonics of ultrashort pulses in laser ablation based materials are related with the higher conversion efficiency. In the meantime, the method of “mild” ablation of graphene, when the structure of material remains intact in the plasma plume, could be the ideal approach for the analysis of the high-order nonlinear optical properties of this medium. In this Letter, we demonstrate for the first time the HHG of femtosecond pulses in the laser ablation plume containing graphene nanoparticles.

The uncompressed radiation of Ti:sapphire laser was used as a heating pulse (central wavelength $\lambda = 802 \text{ nm}$, pulse duration 370 ps, pulse energy $E_{\text{hp}} = 4 \text{ mJ}$) to ablate the target for plasma formation. The heating pulse was focused using the 200 mm focal length cylindrical lens inside the vacuum chamber containing an ablating material to create the extended plasma plume (5 mm) above the target surface (Fig. 1). The intensity of heating pulses on a plain target surface was in the range of $(1-3) \cdot 10^9 \text{ W} \cdot \text{cm}^{-2}$. The compressed driving pulse from the same laser with the energy of $E_{\text{dp}} = 4 \text{ mJ}$ and 64 fs pulse duration was used, after 45 ns delay from the beginning of ablation, for harmonic generation in the plasma plume. This driving pulse was focused using the 400 mm focal length spherical lens onto the extended plasma from the orthogonal direction, at a distance of $\sim 100 \mu\text{m}$ above the target surface. The laser intensity did not change in the laser plasma interaction length since the confocal parameter of focused radiation was 12 mm. The intensity of 802 nm driving pulses at the focus area was varied up to $6 \cdot 10^{14} \text{ W} \cdot \text{cm}^{-2}$ by changing the energy of those pulses. The harmonic emission was analyzed by an extreme ultraviolet (XUV) spectrometer containing a cylindrical mirror and a 1200 grooves/mm flat field grating with variable line spacing. The spec-

¹)e-mail: rashid_ganeev@mail.ru

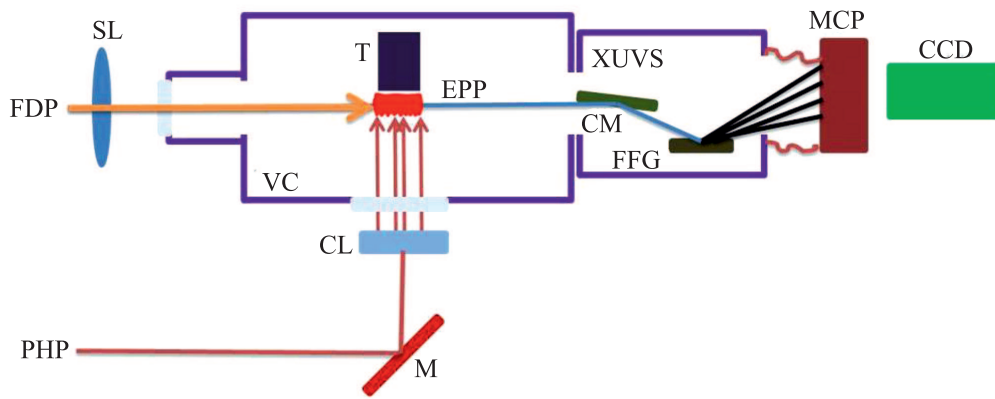


Fig. 1. Experimental scheme for harmonic generation in the extended graphene plasma plume: FDP – femtosecond driving pulse; PHP – picosecond heating pulse; SL – spherical lens; CL – cylindrical lens; M – mirror; VC – vacuum chamber; T – target; EPP – extended plasma plume; XUVS – extreme ultraviolet spectrometer; CM – cylindrical mirror; FFG – flat field grating; MCP – micro-channel plate registrar; CCD – charge coupled device camera

trum was recorded by a micro-channel plate detector with the phosphor screen, which was imaged onto a CCD camera.

We studied graphene nanoparticle powder (SkySpring Nanomaterials Inc.) as the ablating target. To compare the yield of harmonics from cluster-contained and monoparticle-contained plasmas the carbon nanotube (CNT) powder, diamond nanoparticle (DN) powder, and 5-mm-long bulk graphite and bulk silver were used as the targets as well. The powders of above materials were glued on the 5-mm-long glass plates and were installed in the vacuum chamber for ablation. The application of above powdered targets enabled the observation of harmonic generation along a longer wavelength range of XUV (25–80 nm; 11th–33rd harmonics of the 802 nm radiation).

Graphene nanopowders are very thin (5–10 nm in thickness) flat particles with quite large diameters. Like other nanoparticles, the small size gives rise to certain handling issues. In the case of graphene nanoparticles, the ablation plasma plume may contain various species of carbon, i.e. neutrals and ions, small molecules, small and large clusters, aggregates, etc., which can contribute to harmonic generation in various extents. It is important to determine their presence in the region where the driving laser beam interacts with the expanding plasma. Our morphological TEM studies confirmed the presence of relatively large multi-plate graphene species deposited on the nearby substrates at the conditions of the optimal ablation using the 370-ps pulses. Thus, the possible components in the laser heated graphene plume, at 45 ns after laser ablation, when the driving laser pulse interacts with plume, could be the large sheets of fullerenes. We were able observing the monolayer, bi-

layer, trilayer, etc. nanosized chunks depending on the conditions of ablation. However, some uncertainty still remains about the correlation of the presence of different graphene nanoparticles in the carbon plasma and their influence on the nonlinear optical response of medium during harmonic generation. Notice that the time-of-flight mass spectrometry studies of graphene ablated at the conditions similar to those used for HHG showed the presence of small clusters of carbon (C_2 – C_4). We did not observe other ionized clusters, though searched along the wide area of mass-charge units.

Powdered targets are difficult to keep intact for a long time during their continuous ablation. Our studies of the decay of harmonic yield from the graphene plasma were performed at 10 Hz pulse repetition rate, without the movement of target from shot to shot. This led to deterioration of the optimal plasma formation after a few hundred shots on the same place of graphene-contained target. This effect was reported during previous HHG studies using the powdered target ablation [10] and is attributed to the modification of target surface (i.e. evaporation of powder, melting of heated area, modification of surface properties, etc.). To keep stable harmonic yield, one has to move up and down the target holder. Contrary to that, in the case of bulk graphite ablation, the stable harmonic generation was lasted for a considerably longer time. Previous method to hold the stable harmonic emission from plasma was based on the rotation of target (cylindrical rod) and the ablation of its surface using the narrow heating beam [11]. In our case, this method was unacceptable since we used the plain graphene contained target to create the extended graphene plasma. Since the harmonic yield at a given spot on the target became weaker after hundreds

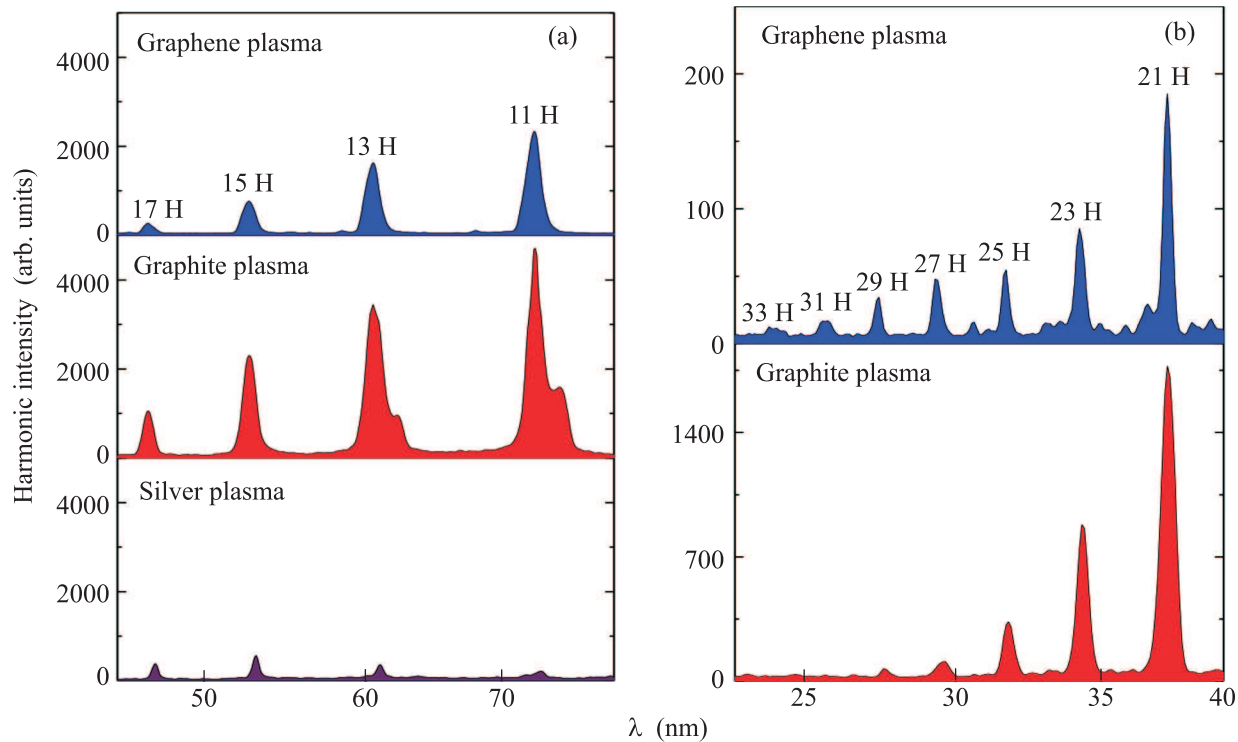


Fig. 2. (a) – Lower-order harmonic spectra from the graphene (upper panel), graphite (middle panel), and silver (bottom panel) plasmas. (b) – Harmonic spectra near the cut-off region from the graphene (upper panel) and graphite (bottom panel) plasmas

of laser shots, this effect was taken into account during the optimization of laser ablation for HHG.

The majority of previous plasma harmonic studies were carried out using the short length plasma plumes ($l \leq 0.5$ mm). One could expect that the application of longer plasmas would enhance the conversion efficiency due to the quadratic dependence of the nonlinear optical response of the medium on the length of laser-matter interaction. To achieve higher HHG conversion efficiency, the length of the medium might be increased provided the phase mismatch between the laser field and the harmonic radiation maintains low. However, once the medium sizes exceed the coherence length, the harmonic intensity will be saturated due to phase mismatch. To analyze this process in the laser-produced plasmas one has to carefully define the best conditions of plasma HHG in the extended medium, while taking into account the peculiar properties of the material used for laser ablation.

The comparative studies of 0.5-mm-long and 5-mm-long graphene plasmas showed the $\sim 7\times$ growth of harmonic yield in the case of extended medium. During these experiments, the 0.5- and 5-mm-long targets were ablated at the same laser power. This enhancement factor of harmonic emission falls short compared with the

expected quadratic growth of harmonic yield with the growth of plasma length ($100\times$), probably due to the growing phase mismatch between the interacting waves at the conditions when the coherence length of those harmonics becomes shorter than the length of extended medium. The analysis of the dependence of harmonic yield on the plasma length showed that the quadratic rule was maintained up to the $l = 3.5$ mm, with further saturation and gradual decrease of harmonic yield. This observation gives a rough estimate of the coherence length for the highest-order harmonics observed in our experiments. Our studies of driving pulse did not show the attenuation after the propagation through the extended graphene plasma plume. This means that neither absorption nor scattering of driving beam play important role during these experiments. The estimated density of plasma was $2 \cdot 10^{17}$ cm $^{-3}$. This relatively low-dense medium did not lead to the attenuation of both driving and harmonic waves.

Fig. 2a shows the low-order harmonic spectra from the graphene, graphite, and silver 5-mm-long plasmas at the conditions of optimal ablation. These conditions correspond to the maximal yields of harmonics in each of above cases. One can see the prevalence of both graphene and graphite plasma harmonics over the

Ag plasma harmonics. We used the graphite and silver plasmas due to known harmonic conversion efficiencies in these media, which allowed the estimation of the photon yield from the graphene plasma (see below).

The harmonic spectra from the graphene plasma in many cases contained the plasma emission at maximal harmonic yields, contrary to the case of graphite ablation when the appearance of strong ionic emission was followed with a deterioration of the optimal plasma conditions for the HHG. In the case of graphene nanopowder ablation, the plasma lines in the longer-wavelength range of spectrum (50–90 nm) were assigned to the singly ionized carbon. The absence of plasma emission from higher charged ions in this spectral range was attributed to the moderate excitation of graphene. The driving pulse also did not cause the appearance of strong spectral lines from the higher-charged carbon ions. The appearance of ionic emission from the ablation of carbon-contained targets in most cases affected the harmonic yield. Our studies of the plasma emission during the over-excitation of the bulk graphite have shown some similarity of this emission with the one from the graphene nanopowder plasma. We also analyzed the availability of harmonic generation during ablation of the pure glue, without the inclusion of graphene clusters. No harmonics were observed in that case. The over-excitation of glue led to plasma formation. The emission in that case was clearly distinguished from the emission generated in the graphene-contained plasma.

Fig. 2b shows the harmonic distribution in the cut-off region in the cases of using the graphene and graphite plasmas. We were able to generate the harmonics in the former plasma up to the 33rd order. The over-excitation of graphene target or the increase of driving pulse intensity (from $3 \cdot 10^{14}$ to $6 \cdot 10^{14}$ W · cm⁻²) did not increase the harmonic cut-off but rather led to the growth of plasma emission and deterioration of the HHG. The shorter wavelength spectra of harmonic emission from the graphene plasma did not show the efficient emission of harmonics above the 33rd order, which points out the prevailing involvement of the singly charged ions, rather than neutral clusters or doubly charged ions, in the harmonic generation. This assumption was based on the ionization potentials of the carbon atom and three-step model of HHG.

The divergence of harmonics was analyzed using the flat mirror installed instead of the cylindrical one in the XUV spectrometer. The comparative studies of harmonic and driving beams showed the fourfold decrease of the divergence in the former case.

Below, we address the usefulness of application of the graphene nanopowder for the efficient harmonic generation. The exact mechanism of the HHG from clusters is still debated, though the harmonic enhancement has been reported using both gas and plasma clusters. The important contribution to the harmonic emission may come from a wave function partially delocalized over the whole cluster, from which electrons tunnel out of and to which they recombine coherently. From an experimental point of view a particular difficulty consists in disentangling the harmonics produced by different species (monomers and clusters of different sizes) and possibly different mechanisms. The practical application of graphene nanopowder is restricted due to the short-lasting stability of harmonic yield in the case of the ablation of the same spot of the target. The comparative measurements of the harmonic yields from graphene, CNT, and DN have shown stronger harmonic emission in the case of diamond nanoparticles. The comparative harmonic spectra from three different clustered plasmas (CNT, DN, and graphene) are shown in the three upper panels of Fig. 3. Here we also show the plasma emission

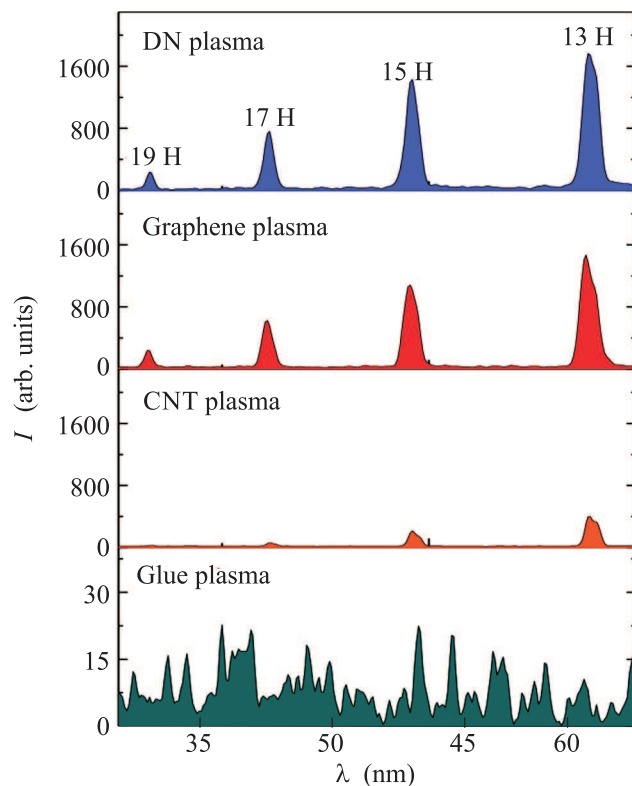


Fig. 3. Low-order harmonic spectra from the DN (upper panel), graphene (second panel), and CNT (third panel) plasmas. Bottom panel shows the plasma spectrum from the ablation of pure glue

observed in the case of the excitation of pure glue, without the insertion of clustered powders of above species. We did not measure the absolute values of the conversion efficiencies of the low-order harmonics from the plasma contained graphene nanopowder, though the ratio between the harmonic yields from this medium and bulk carbon ablation was $\sim 1 : 3$. Taking into account the reported conversion efficiency from the bulk graphite ablation (10^{-4} [12]), the conversion efficiency from the graphene plasma was estimated to be $3 \cdot 10^{-5}$ for the 11th–17th harmonics. The corresponding photon yield of these harmonics was $2 \cdot 10^{10}$ per pulse. Those studies [12] were carried out using the narrow plasma, so we also analyzed the conversion efficiency at similar conditions of plasma formation. We compared our measurements of harmonics from 0.5-mm-long graphene plasma with the absolute measurements of the conversion efficiency in the case of silver plasma using the technique described in [13] and found the similar values of photon yield.

As it was already mentioned, our time-of-flight mass spectrometry measurements showed the presence of small nanoparticles in the laser plasma in the case of ablation of the graphene nanopowder. We did not find higher ionized clusters, though we searched for over a longer range of delays (up to a few tens μs) between the onset of laser ablation and the switching on the triggering pulse in the time-of-flight mass spectrometer. Probably, those large, of the order of a few tens of thousands mass/charge units, clusters were presented in the plasmas as the neutrals.

In conclusion, we have demonstrated the high-order harmonic generation of femtosecond pulses in the laser ablation plume contained the graphene nanoparticles. The harmonics up to the 33rd order were observed. The presence of graphene nanoparticles in the laser plasma was confirmed during the analysis of ablation debris.

This work was supported by JSPS KAKENHI (grant #24760048). The authors are grateful to Prof. Y. Sakamoto and Division of Analytical Science, Biomedical Research Centre, Saitama Medical School for time-of-flight mass spectrometry and TEM measurements.

-
1. K. Geim and K. S. Novoselov, *Nat. Mat.* **6**, 183 (2007).
 2. S. A. Mikhailov, *Phys. Rev. B* **84**, 045432 (2011).
 3. S. Wu, L. Mao, A. M. Jones, W. Yao, C. Zhang, and X. Xu, *Nano Lett.* **12**, 2032 (2012).
 4. M. Gullans, D. E. Chang, F. H. L. Koppens, F. J. García de Abajo, and M. D. Lukin, *Phys. Rev. Lett.* **111**, 247401 (2013).
 5. S. A. Sørngård, S. I. Simonsen, and J. P. Hansen, *Phys. Rev. A* **87**, 053803 (2013).
 6. E. Hendry, P. J. Hale, J. Moger, and A. K. Savchenko, *Phys. Rev. Lett.* **105**, 097401 (2010).
 7. K. L. Ishikawa, *Phys. Rev. B* **82**, 201402 (2010).
 8. R. A. Ganeev, L. B. Elouga Bom, J. Abdul-Hadi, M. C. H. Wong, J. P. Brichta, V. R. Bhardwaj, and T. Ozaki, *Phys. Rev. Lett.* **102**, 013903 (2009).
 9. R. A. Ganeev, P. A. Naik, H. Singhal, J. A. Chakera, M. Kumar, M. P. Joshi, A. K. Srivastava, and P. D. Gupta, *Phys. Rev. A* **83**, 013820 (2011).
 10. R. A. Ganeev, C. Hutchison, M. Castillejo, I. Lopez-Quintas, F. McGrath, D. Y. Lei, and J. P. Marangos, *Phys. Rev. A* **88**, 033803 (2013).
 11. C. Hutchison, R. A. Ganeev, T. Witting, F. Frank, W. A. Okell, J. W. G. Tisch, and J. P. Marangos, *Opt. Lett.* **37**, 2064 (2012).
 12. L. B. Elouga Bom, Y. Pertot, V. R. Bhardwaj, and T. Ozaki, *Opt. Express* **19**, 3077 (2011).
 13. R. A. Ganeev, M. Baba, M. Suzuki, and H. Kuroda, *Phys. Lett. A* **339**, 103 (2005).